

See discussions, stats, and author profiles for this publication at: <https://www.researchgate.net/publication/276208419>

# Interfacial Synthesis of Two-Dimensional Dendritic Platinum Nanoparticles Using Oleic Acid-in-Water Emulsion

ARTICLE in ACS APPLIED MATERIALS & INTERFACES · MAY 2015

Impact Factor: 6.72 · DOI: 10.1021/acsmami.5b02433 · Source: PubMed

---

CITATION

1

READS

26

## 5 AUTHORS, INCLUDING:



David Minzae Lee  
Seoul National University  
11 PUBLICATIONS 132 CITATIONS

[SEE PROFILE](#)



Taewook Kang  
Sogang University  
64 PUBLICATIONS 1,301 CITATIONS

[SEE PROFILE](#)

# Interfacial Synthesis of Two-Dimensional Dendritic Platinum Nanoparticles Using Oleic Acid-in-Water Emulsion

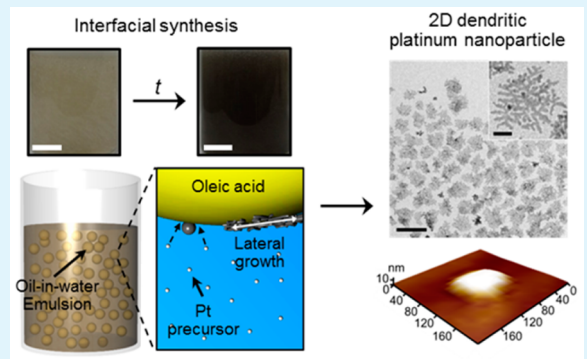
Eui-Geun Jung,<sup>†,‡</sup> Yonghee Shin,<sup>†,‡</sup> Minzae Lee,<sup>§</sup> Jongheop Yi,<sup>§</sup> and Taewook Kang<sup>\*,†</sup>

<sup>†</sup>Department of Chemical and Biomolecular Engineering, Sogang University, Seoul 121-742, Korea

<sup>§</sup>School of Chemical and Biological Engineering, Institute of Chemical Processes, Seoul National University, Seoul 151-742, Korea

## Supporting Information

**ABSTRACT:** Here we propose facile and scalable synthesis of two-dimensional (2D) dendritic platinum nanoparticle at room temperature by exploiting an oil-in-water emulsion. The interfacial synthesis selectively provides platinum nanoparticle with 2D structure in high yield by controlling key reactants such as the amount of oleic acid and the concentration of block copolymer. Electrocatalytic activity of 2D dendritic platinum nanoparticle for oxygen reduction and methanol oxidation reaction is also examined.



**KEYWORDS:** *interfacial synthesis, dendritic platinum nanoparticle, two-dimensional structure, oil-in-water emulsion, electrocatalytic activity*

Platinum nanoparticles have attracted considerable attention because of their high catalytic performance in a wide variety of applications ranging from fine-chemical synthesis to energy harvesting.<sup>1–5</sup> Many studies have been focused on the synthesis of platinum nanoparticles with tunable size and shape to further improve their physicochemical properties. Consequently, platinum nanoparticles with various shapes such as sphere,<sup>6</sup> cube,<sup>7,8</sup> polyhedron,<sup>9,10</sup> mesoporous structure,<sup>11</sup> and wire<sup>12,13</sup> have been reported to show high catalytic performance. Among the platinum nanoparticles, those with dendritic structure would offer several key advantages such as high surface-to-volume ratio and numerous absorption sites that are available for catalytic reactions without diffusion limitation.<sup>14,15</sup>

To date, the proposed synthetic techniques for such dendritic nanoparticles rely on either thermal decomposition of platinum precursors<sup>16–18</sup> or physical sacrificial templates.<sup>19,20</sup> However, thermal decomposition is typically carried out at high temperatures and needs delicate temperature control during synthesis, and the template-based method requires additional steps for the preparation and removal of the template, making scale-up for industrial applications difficult.

Here we report room-temperature, facile, and scalable synthesis of two-dimensional (2D) dendritic platinum nanoparticle using an oleic acid-in-water emulsion. Interestingly, this immiscible liquid/liquid interface produces the nanoparticle with 2D dendritic structure and large accessible surface area for neighboring reactants without diffusion limitation. 2D dendritic platinum nanoparticle can be selectively obtained in high yield by controlling the amount of oleic acid and the concentration

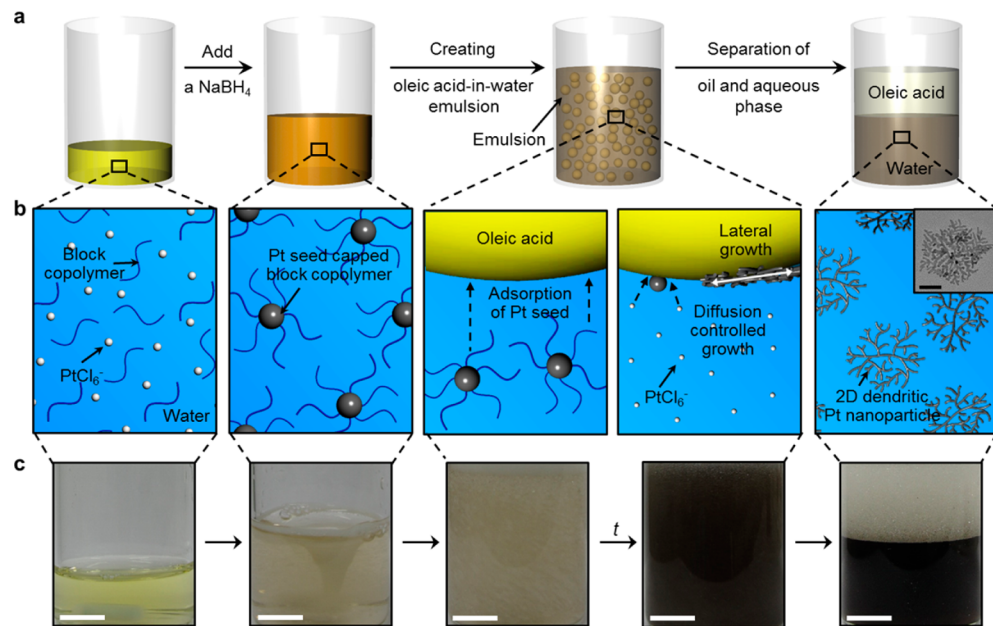
of block copolymers. In addition, electrocatalytic activity of the nanoparticle in oxygen reduction reaction and in methanol oxidation reaction is studied.

Figure 1 presents a schematic illustration of the experimental procedure for the interfacial synthesis of 2D dendritic platinum nanoparticle (DPN) at room temperature. In brief,  $H_2PtCl_6$  aqueous solution containing the triblock copolymer poly(ethylene oxide)-poly(propylene oxide)-poly(ethylene oxide) ( $PEO_{100}-PPO_{65}-PEO_{100}$ , Pluronic F127) was prepared, and the reducing agent,  $NaBH_4$ , was then added to the solution. We observed that the color of the solution immediately changed to light brown (Figure 1c), indicating the formation of small platinum seeds. Oleic acid was then introduced into the solution with vigorous stirring to create an emulsion. As the reaction proceeded, the color of the emulsion gradually changed to brownish black (Figure 1c), which is indicative of the growth of platinum nanoparticle in the oleic acid-in-water emulsion system. Because of difference in densities of oil and water, the emulsion was easily separated into oleic acid and a brownish black aqueous phase after the reaction. The absence of an absorbance peak for the platinum precursor (i.e.,  $H_2PtCl_6$ ) after 30 min shows the complete reduction of the precursor (Figure S1a in the Supporting Information).

To characterize as-synthesized platinum nanoparticle, the aqueous phase was sampled by centrifugation (three times) to

Received: March 19, 2015

Accepted: May 12, 2015



**Figure 1.** (a, b) Schematic illustration of the interfacial synthesis of two-dimensional dendritic platinum nanoparticle using an oleic acid-in-water emulsion at room temperature. (c) Photographs corresponding to each experimental step. Scale bar = 1 cm (c) and 25 nm (TEM image in b).

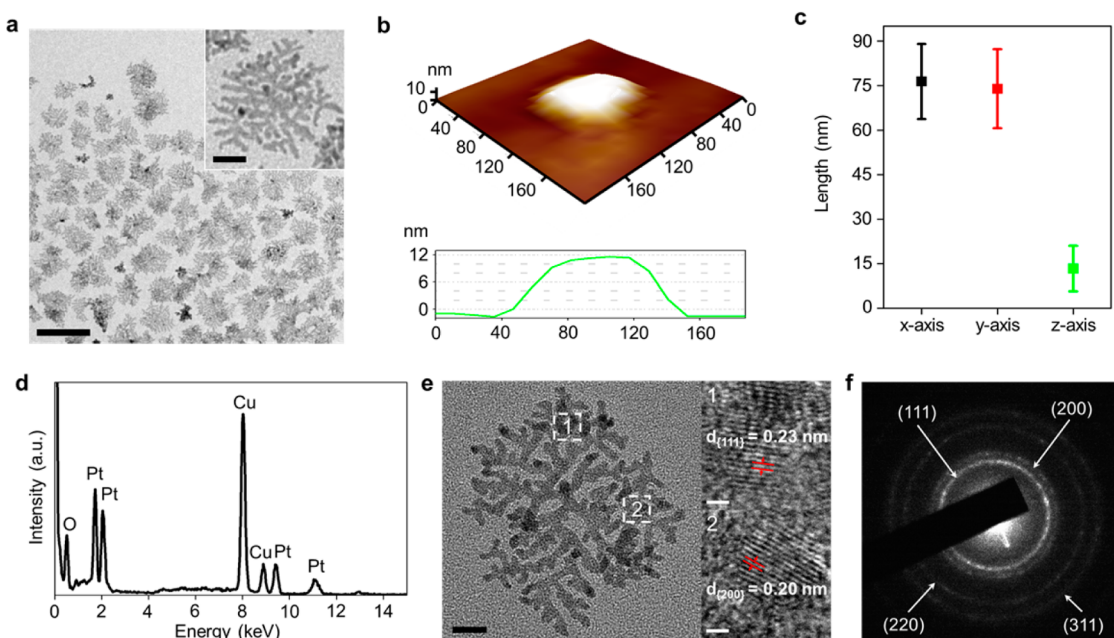


**Figure 2.** Characterization of platinum nanoparticle synthesized in an oleic acid-in-water emulsion. (a) TEM images of particles sampled from the aqueous phase. (b) Typical image and thickness profile of a particle measured under an atomic force microscope. (c) Statistical analysis results for the lateral size (x, y-axis) and thickness (z-axis). (d) EDS spectrum, (e) high-resolution TEM images, and (f) SAED pattern. Scale bars are (a) 100 nm and (inset) 20 nm; (e) 10 nm and (inset) 1 nm.

remove the reactants. Figure 2a shows representative transmission electron microscope (TEM) images of the nanoparticle obtained from the emulsion. The platinum nanoparticle clearly has a dendritic structure with many small branches (inset of Figure 2a). To statistically analyze their lateral sizes, 100 particles in a microscope image are randomly selected. The average lateral sizes with respect to the x- and y-axes of the particles are found to be  $76.3 \pm 12.6 \text{ nm}$  and  $73.9 \pm 13.3 \text{ nm}$  (Figure 2c), respectively. The thicknesses of the particles were measured under an atomic force microscope, as shown in Figure 2b. The average thickness of  $13.3 \pm 7.6 \text{ nm}$  (Figure 2c)

suggests that the nanoparticles are quite 2D. Energy-dispersive X-ray spectroscopy (EDS) of 2D DPN was also performed. EDS spectrum shows the peaks that are assigned to platinum (Figure 2d). EDS spectrum presents the peak that corresponds to oxygen (Figure 2d), indicating the existence of the oleic acid at the surface of 2D DPN before washing. We obtained EDS spectrum after washing with ethanol. EDS spectrum shows that the peak intensity of oxygen after washing is dramatically decreased (Figure S2 in the Supporting Information), indicating the complete desorption of the oleic acid. Note that additional peaks in EDS spectra are originated from a

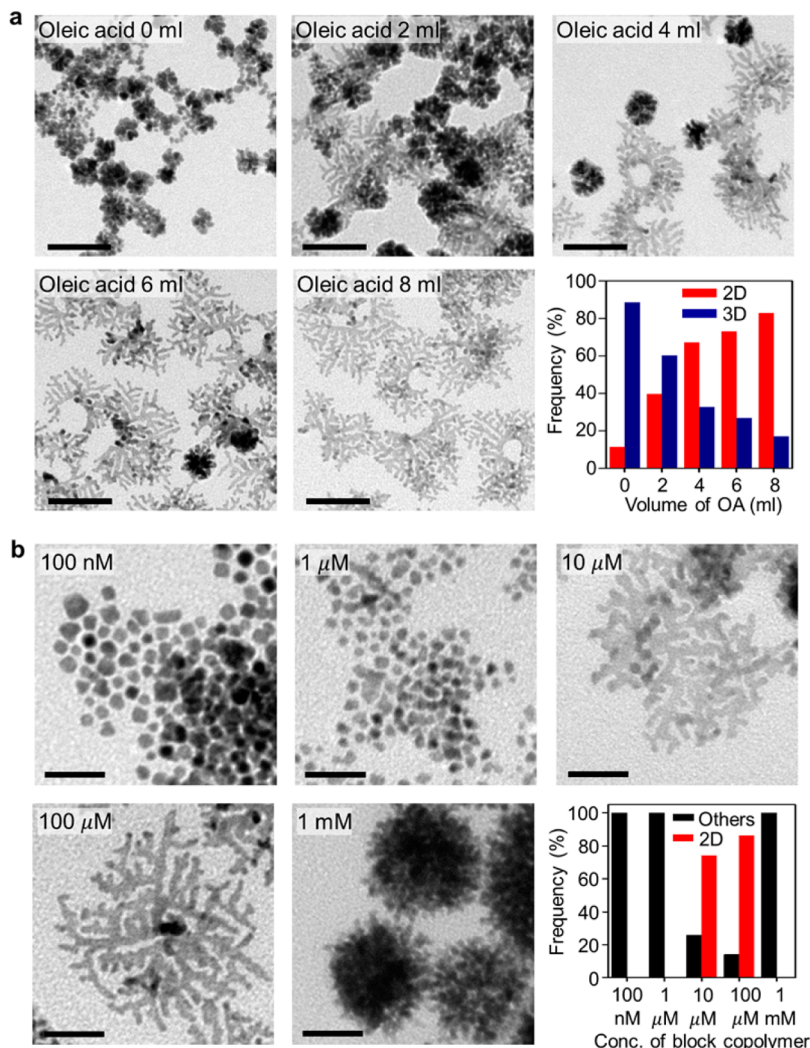


**Figure 3.** (a) TEM images showing the effect of the amount of oleic acid on the structure of platinum nanoparticle and shape distribution with respect to the 2D nanoparticle (red) corresponds to light-gray particles in the TEM image, and three-dimensional nanoparticle (blue) correspond to dark-gray particles formed according to amounts of added oleic acid used for forming an emulsion. The amounts of oleic acid are 0, 2, 4, 6, and 8 mL, respectively. (b) TEM images showing the effect of PEO<sub>100</sub>-PPO<sub>65</sub>-PEO<sub>100</sub> block copolymer concentration on the particle shape and shape distribution with respect to the 2D dendritic nanoparticle (red) and others (e.g., spherical and 3D dendritic structure) (black). The concentrations of the block copolymer are 100 nM and 1, 10, 100 μM, and 1 mM, respectively. Scale bars = (a) 50 and (b) 20 nm.

copper grid. High-resolution TEM images of 2D DPN are captured to identify the crystalline structure (Figure 2e). The calculated lattice spacing is 0.23 nm (1 in Figure 2e) and 0.20 nm (2 in Figure 2e) which correspond to lattice characteristics of {111} and {200} planes of typical face-centered cubic (FCC) lattice, respectively.<sup>21,22</sup> In addition, selected area electron diffraction (SAED) pattern of the particle was obtained. SAED pattern shows circular rings corresponding to {111}, {200}, {220} and {311} planes of FCC lattice (Figure 2f), indicating polycrystalline nature of 2D DPN.

To further elaborate the interfacial synthesis, we explored the effect of the amount of oleic acid on the final structure of the nanoparticle obtained from the emulsion by changing the volume of added oleic acid from 0 to 8 mL. The selectivity for 2D dendritic nanoparticle in the absence of oleic acid is found to be only 11.4% (Figure 3a). As the volume of oleic acid is increased, the selectivity drastically increases up to 82.9% (Figure 3a).

Because the block copolymer would stabilize both small platinum seed and large 2D nanoparticle,<sup>23–25</sup> we also

examined the effect of PEO<sub>100</sub>-PPO<sub>65</sub>-PEO<sub>100</sub> block copolymer on the growth of nanoparticle by varying its concentration from 100 nM to 1 mM. At low concentrations (100 nM and 1 μM), aggregates of numerous spherical nanoparticles with around 10 nm diameter (Figure 3b) are mainly observed. Note that at low concentrations, the color of oleic acid changed to black, indicating the diffusion of nanoparticles into the oleic acid layer (Figure S1b in the Supporting Information). With increasing the concentration of the block copolymer (10 μM and 100 μM), the number of particle with 2D dendritic shape increases (Figure 3b). Upon further increases in the concentration to above the critical micelle concentration, three-dimensional nanoparticle with small branches is found to be formed (1 mM in Figure 3b).

On the basis of these experimental observations, we postulate the reaction mechanism for the formation of 2D DPN under the given experimental conditions as following: (1) amphiphilic block copolymer that would cap small platinum seeds with around 10 nm diameter,<sup>24</sup> is likely to be adsorbed onto the immiscible interface between oleic acid and water.<sup>26–28</sup> (2)

Because the interface can provide diffusion-controlled growth conditions driven by the attraction of platinum precursors to the carboxyl headgroup of oleic acid,<sup>29,30</sup> small seeds would undergo further structural evolution to larger 2D dendritic nanoparticle at the interface.

To examine the electrocatalytic activity of 2D DPN, we carried out an oxygen reduction reaction. Cyclic voltammetry (CV) plots of 2D DPN before and after washing with ethanol exhibit two characteristic potential regions (Figure 4a) that

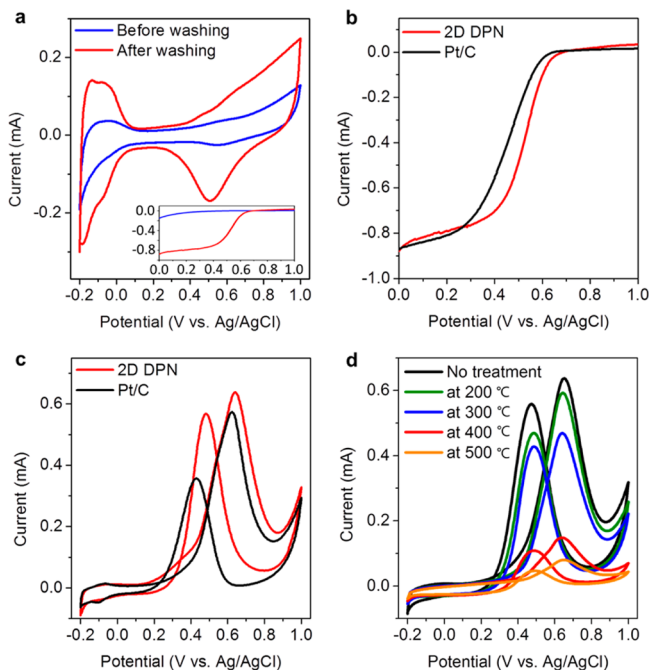


**Figure 4.** (a) Cyclic voltammetry (CV) plots of 2D dendritic platinum nanoparticle (DPN) before (blue) and after (red) washing with ethanol in N<sub>2</sub>-saturated 0.1 M HClO<sub>4</sub> aqueous solution. Linear-sweep voltammetry (LSV) curves of 2D DPN before and after washing in oxygen reduction reaction (inset). (b) LSV curves of 2D DPN washed with ethanol (red) and Pt/C (black) in O<sub>2</sub>-saturated 0.1 M HClO<sub>4</sub> aqueous solution. (c) CV plots of 2D DPN washed with ethanol (red) and Pt/C (black) and (d) CV plots of 2D DPN subjected to heat treatment at different temperatures in a N<sub>2</sub>-saturated 0.5 M H<sub>2</sub>SO<sub>4</sub> aqueous solution containing 1 M methanol. The scan rate was 50 mV/s.

correspond to the hydrogen adsorption/desorption in the range  $-0.2$  and  $0.1$  V, and the platinum oxidation from  $0.2$  to  $0.8$  V, respectively. Compared to 2D DPN before washing, the peak current is significantly increased after washing. The electrochemical active surface area (EASA) is also calculated by the hydrogen adsorption/desorption based on the CV data (Table S1 in the Supporting Information). The EASA of 2D DPN is increased by 5 times after washing (from  $14.26$  to  $71.24$  m<sup>2</sup>/g). Linear-sweep voltammetry (LSV) curves (inset Figure 4a) show that the onset potential of 2D DPN after washing with ethanol is  $0.69$  V, while the nanoparticle before washing does not show any considerable change due to oleic acid physisorbed on the surface of the particle. For a comparison, commercially available carbon-supported Pt catalyst (Pt/C, 20 wt % Pt, platinum nanoparticles on carbon black, mean diameter of platinum particle  $\approx 3.4$  nm) was tested in oxygen reduction reaction. LSV curves in Figure 4b show that the onset potential of our 2D DPN ( $0.69$  V) is higher than that of Pt/C ( $0.65$  V).

Next, methanol oxidation reaction was also examined. CV plots (Figure 4c) show that the peak in the forward scan of the 2D DPN ( $0.64$  V) is slightly higher than the Pt/C ( $0.62$  V) and the backward scan produces a similar result (2D DPN:  $0.48$  V, Pt/C:  $0.43$  V). In addition, the peak currents in both the forward and backward scans of our 2D nanoparticle are higher than those of Pt/C (2D DPN:  $0.64$  and  $0.56$  mA, Pt/C:  $0.57$  and  $0.36$  mA). We further investigated the change in the electrocatalytic activity by annealing 2D DPN. As shown in Figure S3 in the Supporting Information, the morphology of the particle changes from dendrite to aggregate as the annealing temperature increases, indicating that the surface-to-volume ratio of the nanoparticles markedly decreases. CV plots in Figure 4d show that as the annealing temperature increases, peak currents in the forward scan at  $0.64$  V of the annealed nanoparticles decrease from  $0.64$  to  $0.08$  mA. A similar decrease in peak currents in the backward scan at  $0.49$  V (from  $0.56$  to  $0.05$  mA) is also observed.

In conclusion, we have demonstrated that an oleic acid-in-water emulsion can be utilized to prepare 2D dendritic platinum nanoparticle at room temperature. Both the amount of oleic acid and the concentration of block copolymer (PEO<sub>100</sub>-PPO<sub>65</sub>-PEO<sub>100</sub>) play an important role in the formation of the resulting 2D dendritic nanoparticle. The 2D dendritic platinum nanoparticle exhibits higher electrocatalytic activities for oxygen reduction reaction and methanol oxidation reaction than commercial Pt/C. Annealing 2D dendritic platinum nanoparticle reduces electrocatalytic activity for the methanol oxidation reaction because of the decrease in the surface-to-volume ratio.

## ASSOCIATED CONTENT

### Supporting Information

Experimental details including materials and methods, UV-visible spectrum and photographs of the reaction solution, EDS spectra of platinum nanoparticles after washing, TEM images and EDS spectra of platinum nanoparticles with heat treatment, and calculated EASA data. The Supporting Information is available free of charge on the ACS Publications website at DOI: 10.1021/acsami.5b02433.

## AUTHOR INFORMATION

### Corresponding Author

\*E-mail: twkang@sogang.ac.kr

### Author Contributions

<sup>†</sup>E.-G.J. and Y.S. contributed equally.

### Notes

The authors declare no competing financial interest.

## ACKNOWLEDGMENTS

This research was supported by the Human Resources Development program (No. 20114010203090) of the Korea Institute of Energy Technology Evaluation and Planning (KETEP) grant funded by the Korea government Ministry of Trade, Industry and Energy and the International Research & Development Program of the National Research Foundation of Korea (NRF) funded by the Ministry of Science, ICT & Future Planning (No. 2013K1A3A1A32035444).

## ABBREVIATIONS

2D, two-dimensional

$\text{PEO}_{100}\text{-PPO}_{65}\text{-PEO}_{100}$ , poly(ethylene oxide)-poly(propylene oxide)-poly(ethylene oxide)  
DPN, dendritic platinum nanoparticle

## ■ REFERENCES

- (1) Yu, T.; Kim, D. Y.; Zhang, H.; Xia, Y. Platinum Concave Nanocubes with High-Index Facets and Their Enhanced Activity for Oxygen Reduction Reaction. *Angew. Chem., Int. Ed.* **2011**, *50*, 2773–2777.
- (2) Sun, S.; Zhang, G.; Geng, D.; Chen, Y.; Li, R.; Cai, M.; Sun, X. A Highly Durable Platinum Nanocatalyst for Proton Exchange Membrane Fuel Cells: Multiarmed Starlike Nanowire Single Crystal. *Angew. Chem.* **2011**, *123*, 442–446.
- (3) Preze-Alonso, F. J.; McCarthy, D. N.; Nierhoff, A.; Hernandez-Fernandez, P.; Strelbel, C.; Stephens, I. E. L.; Nielsen, J. H.; Chorkendorff, I. The Effect of Size on the Oxygen Electroreduction Activity of Mass-Selected Platinum Nanoparticles. *Angew. Chem., Int. Ed.* **2012**, *51*, 4641–4643.
- (4) Mourdikoudis, S.; Chirea, M.; Altantzis, T.; Pastoriza-Santos, I.; Perez-Juste, J.; Silva, F.; Bals, S.; Liz-Marzan, L. M. Dimethylformamide-Mediated Synthesis of Water-Soluble Platinum Nanodendrites for Ethanol Oxidation Electrocatalysis. *Nanoscale* **2013**, *5*, 4776–4784.
- (5) Dasgupta, N. P.; Liu, C.; Andrews, S.; Prinz, F. B.; Yang, P. Atomic Layer Deposition of Platinum Catalysts on Nanowire Surfaces for Photoelectrochemical Water Reduction. *J. Am. Chem. Soc.* **2013**, *135*, 12932–12935.
- (6) Bigall, N. C.; Hartling, T.; Klose, M.; Simon, P.; Eng, L. M.; Eychmuller, A. Monodisperse Platinum Nanospheres with Adjustable Diameters from 10 to 100 nm: Synthesis and Distinct Optical Properties. *Nano Lett.* **2008**, *8*, 4588–4592.
- (7) Chiu, C.; Li, Y.; Ruan, L.; Ye, X.; Murray, C. B.; Huang, Y. Platinum Nanocrystals Selectively Shaped Using Facet-Specific Peptide Sequences. *Nat. Chem.* **2011**, *24*, 393–399.
- (8) Forbes, L. M.; Goodwin, A. P.; Cha, J. N. Tunable Size and Shape Control of Platinum Nanocrystals from a Single Peptide Sequence. *Chem. Mater.* **2010**, *22*, 6524–6528.
- (9) Tian, N.; Zhou, Z.-Y.; Sun, S.; Ding, Y.; Wang, Z. L. Synthesis of Tetrahedral Platinum Nanocrystals with High-Index Facets and High Electro-Oxidation Activity. *Science* **2007**, *316*, 732–735.
- (10) Huang, X.; Zhao, Z.; Fan, J.; Tan, Y.; Zheng, N. Amine-Assisted Synthesis of Concave Polyhedral Platinum Nanocrystals Having {411} High-Index Facets. *J. Am. Chem. Soc.* **2011**, *133*, 4718–4721.
- (11) Yamauchi, Y.; Takai, A.; Komatsu, M.; Sawada, M.; Ohsuna, T.; Kuroda, K. Vapor Infiltration of a Reducing Agent for Facile Synthesis of Mesoporous Pt and Pt-Based Alloys and Its Application for the Preparation of Mesoporous Pt Microrods in Anodic Porous Membranes. *Chem. Mater.* **2008**, *20*, 1004–1011.
- (12) Xia, B. Y.; Wu, H. B.; Yan, Y.; Lou, X. W.; Wang, X. Ultrathin and Ultralong Single-Crystal Platinum Nanowire Assemblies with Highly Stable Electrocatalytic Activity. *J. Am. Chem. Soc.* **2013**, *135*, 9480–9485.
- (13) Lee, H.-B.-R.; Baeck, S.; Jaramilo, T. F.; Bent, S. F. Growth of Pt Nanowires by Atomic Layer Deposition on Highly Ordered Pyrolytic Graphite. *Nano Lett.* **2013**, *13*, 457–463.
- (14) Shen, Q.; Jiang, L.; Zhang, H.; Min, Q.; Hou, W.; Zhu, J.-J. Three-dimensional Dendritic Pt Nanostructures: Sonoelectrochemical Synthesis and Electrochemical Applications. *J. Phys. Chem. C* **2008**, *112*, 16385–16392.
- (15) Wang, L.; Yamauchi, Y. Facile Synthesis of Three-Dimensional Dendritic Platinum Nanoelectrocatalyst. *Chem. Mater.* **2009**, *21*, 3562–3569.
- (16) Teng, X.; Liang, X.; Maksimuk, S.; Yang, H. Synthesis of Porous Platinum Nanoparticles. *Small* **2006**, *2*, 249–253.
- (17) Zhong, X.; Feng, Y.; Lieberwirth, I.; Knoll, W. Facile Synthesis of Morphology-Controlled Platinum Nanocrystals. *Chem. Mater.* **2006**, *18*, 2468–2471.
- (18) Mahmoud, M. A.; Tabor, C. E.; El-Sayed, M. A.; Ding, Y.; Wang, Z. L. A New Catalytically Active Colloidal Platinum Nanocatalyst: The Multiarmed Nanostar Single Crystal. *J. Am. Chem. Soc.* **2008**, *130*, 4590–4591.
- (19) Song, Y.; Yang, Y.; Medforth, C. J.; Pereira, E.; Singh, A. K.; Xu, H.; Jiang, Y.; Brinker, C. J.; Swol, F. V.; Shelnutt, J. A. Controlled Synthesis of 2-D and 3-D Dendritic Platinum Nanostructures. *J. Am. Chem. Soc.* **2004**, *126*, 635–645.
- (20) Song, Y.; Hickner, M. A.; Challa, S. R.; Dorin, R. M.; Garcia, R. M.; Wang, H.; Jiang, Y. B.; Li, P.; Qiu, Y.; Swol, F. V.; Medforth, C. J.; Miller, J. E.; Nwoga, T.; Kawahara, K.; Li, W.; Shelnutt, J. A. Evolution of Dendritic Platinum Nanosheets into Ripening-Resistant Holey Sheets. *Nano Lett.* **2009**, *9*, 1534–1539.
- (21) Sun, S. H.; Yang, D. Q.; Villers, D.; Zhang, G. X.; Sacher, E.; Dodelet, J. P. Template- and Surfactant-free Room Temperature Synthesis of Self-Assembled 3D Pt Nanoflowers from Single-Crystal Nanowires. *Adv. Mater.* **2008**, *20*, 571–574.
- (22) Tian, N.; Zhou, Z. Y.; Sun, S. G.; Ding, Y.; Wang, Z. L. Synthesis of tetrahedral platinum nanocrystals with high-index facets and high electro-oxidation activity. *Science* **2007**, *316*, 732–735.
- (23) Sakai, T.; Alexandridis, P. Mechanism of Gold Metal Ion Reduction, Nanoparticle Growth and Size Control in Aqueous Amphiphilic Block Copolymer Solutions at Ambient Conditions. *J. Phys. Chem. B* **2005**, *109*, 7766–7777.
- (24) Niesz, K.; Grass, M.; Somorjai, G. A. Precise Control of the Pt Nanoparticle Size by Seeded Growth Using  $\text{EO}_{13}\text{PO}_{30}\text{EO}_{13}$  Triblock Copolymers as Protective Agents. *Nano Lett.* **2005**, *5*, 2238–2240.
- (25) Wang, L.; Yamauchi, Y. Block Copolymer Mediated Synthesis of Dendritic Platinum Nanoparticles. *J. Am. Chem. Soc.* **2009**, *131*, 9152–9153.
- (26) Akartuna, I.; Studart, A. R.; Tervoort, E.; Gonzenbach, U. R.; Gauckler, L. J. Stabilization of Oil-in-Water Emulsions by Colloidal Particles Modified with Short Amphiphiles. *Langmuir* **2008**, *24*, 7161–7168.
- (27) Saleh, N.; Phenrat, T.; Sirk, K.; Dufour, B.; Ok, J.; Sarbu, T.; Matyjaszewski, K.; Tilton, R. D.; Lowry, G. V. Adsorbed Triblock Copolymers Deliver Reactive Iron Nanoparticles to the Oil/Water Interface. *Nano Lett.* **2005**, *5*, 2489–2494.
- (28) Du, B.; Chen, X.; Zhao, B.; Mei, A.; Wang, Q.; Xu, J.; Fan, Z. Interfacial Entrapment of Noble Metal Nanoparticles and Nanorods Capped with Amphiphilic Multiblock Copolymer at A Selective Liquid–Liquid Interface. *Nanoscale* **2010**, *2*, 1684–1689.
- (29) Plomp, A. J.; Su, D. S.; de Jong, K. P.; Bitter, J. H. On the Nature of Oxygen-Containing Surface Groups on Carbon Nanofibers and Their Role for Platinum Deposition-An XPS and Titration Study. *J. Phys. Chem. C* **2009**, *113*, 9865–9869.
- (30) Wu, B.; Hu, D.; Kuang, Y.; Yu, Y.; Zhang, X.; Chen, J. High Dispersion of Platinum–Ruthenium Nanoparticles on the 3,4,9,10-Perylene Tetracarboxylic Acid-Functionalized Carbon Nanotubes for Methanol Electro-Oxidation. *Chem. Commun.* **2011**, *47*, 5253–5255.